FRACTURE OF LIGHTWEIGHT STRUCTURES BASED ON A COMBINATION OF ENERGY RELEASE RATE BALANCE AND A COHESIVE LAW

Efstathios E. Theotokoglou[1] and Ilias Tourlomousis[2]

[1,] Department of Mechanics, Laboratory of Testing and Materials,
School of Applied Mathematical and Physical Sciences,
National Technical University of Athens, GR-15773 Athens, Greece
e-mail: stathis@central.ntua.gr ; web page: http://users.ntua.gr/stathis

[2] Department of Mechanics, Laboratory of Testing and Materials,
School of Applied Mathematical and Physical Sciences,
National Technical University of Athens, GR-15773 Athens, Greece
ilst@otenet.gr

Keywords: Cohesive law, Critical Energy Release Rate, Damage initiation, Cracking Propagation, Computational Analysis.

Abstract. *This study is an effort to combine the conventional approach of energy release rate and the theory of cohesive law with the application of the finite element procedure in order to simulate the crack initiation - propagation and finally collapse of a lightweight sandwich beam under flexural loading. In the absence of laboratory data it is developed a computational procedure based on Finite Element Analysis to estimate the critical energy release rate values and then introduce them as material constants in a cracked model which is subjected in flexural loading. The whole study uses commercial Abaqus code – codes in Python and Matlab.*

1 INTRODUCTION

When a solid is fractured new surfaces are created within the medium in a thermodynamically irreversible manner. Material separation is caused by the rupture of atomic bonds due to high local stresses. There are two different approaches regarding the analysis of fracture. Both depend on the scale of analysis. First the atomic level which studies phenomena taking place within distances of order of 10^{-7} cm and second -which is our case- the continuum mechanics approach where the distances are of order greater than 10^{-2}cm.

Sandwich structures are more and more implemented in modern industrial applications such as ship hulls wind turbine blades and aerospace applications where low weight and high rigidity is very important. A sandwich material consists of a core material with thin laminate on each side. The laminate could be any combination of fibres and matrices, or even of a metallic material. The core is usually made of PVC, wood or a honeycomb material. The most interesting problems which appeared in sandwich structures are the failures modes in the core and the faces materials, the fracture of the core material and the interaction between the fractured core and the face materials. In sandwich structures the foam is typically the weakest part and it is the first to fail under static or cyclic loading because it transfers the applied loads as shear stresses. In addition a very critical problem in sandwich structures is the debonding problem between the face and core materials [1-5]. Unstable cracking propagation and kinking into the core material represents one of the weakest failure modes in sandwich composites. The fracture behavior in sandwich composites has been directed toward the understanding of crack propagation, and at the same time toward improving the durability of composites against fracture. A crack flaw may be introduced during processing or subsequent service conditions [1-3]. It may result from low velocity impact, from eccentricities in the structural load path, or from discontinuities in structures, which induce a significant out-of-plane stress.

Cohesive crack models are widely used to simulate crack growth and kinking phenomena. The basic concept of cohesive zone was introduced by Barenblatt [6] and Dugdale [7] but Xu and Needlemen [8] introduced the cohesive surface network. In order to develop numerical methodologies to simulate crack propagation in composite structures, cohesive damage models have attracted much interest [9-15] due to their well established advantages compared to the stress based and fracture mechanics methods. But the application of cohesive damage models in sandwich structures for the numerical simulation of the crack propagation is very limited [12-14].

The sandwich beam considered is shown in Figure 1. Material properties and geometrical data are shown in

Tables 1 and 2 respectively. Additional information regarding material properties as shear and tensile strength, are given in Table 3. In this study combining the energy release rate approach with a cohesive law the crack propagation inside the core of a sandwich beam very close to the upper skin interface, is confronted via the finite element analysis [15].

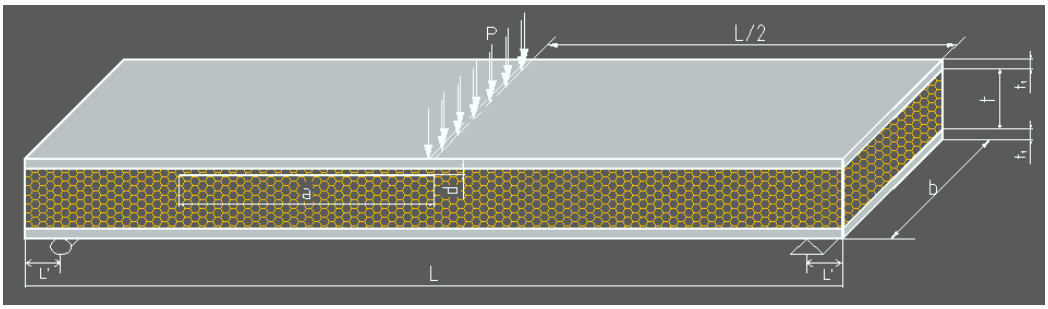

Figure 1: The model of the fractured sandwich beam and the applied loading.

Material	E (MPa)	Poisson ratio ν
Upper and Lower material Layers (isotropic glass reinforced)	16300	0.3
Core material (PVC foam , R75 by DIAB[2])	80	0.4

Table 1 : Material data of the beam [2]

Length, L(mm)	228.6
Width,b(mm)	63.5
Width of the upper and lower layer t_1,t_2 (mm)	2.28
Distance of support from edges L´ (mm)	5
Crack length a (mm)	2,5,10,20,30,40,50,60,70
Distance of crack from the upper face sheet ,d (mm)	1

Table 2: Geometrical data of the beam

Density : (kg/m^3)	75.3
Compressive strength (Mpa)	1.1
Compressive modulus (Mpa)	38
Tensile Strength (Mpa)	2
Tensile Modulus(Mpa)	62
Shear Strength (Mpa)	0.9
Shear Modulus (Mpa)	29

Table 3: Mechanical properties of R-75 [2]

2 THEORETICAL BACKGROUND

2.1 Energy Balance during crack growth

According to the conservation law of energy in a deformable body subjected to arbitrary loading with a crack

embedded, we have [16-18]:

$$\dot{W} = \dot{E} + \dot{K} + \dot{\Gamma}, \tag{1}$$

where $\dot{W}$ is the work performed per unit time by the applied loads, $\dot{E}$ and $\dot{K}$ are the rates of change of the internal energy and kinetic energy of the body and $\dot{\Gamma}$ is the energy per unit spent in increasing the crack area A. The dot over the symbol denotes differentiation with respect to time. The internal energy E can be formed as:

$$E = U^e + U^p, \tag{2}$$

where U^e represents the elastic strain energy and U^p the plastic work. If the applied loads are time independent and the crack grows slowly the kinetic energy term is negligible and can be omitted from (1).We assume that all changes in energy are caused by the change in crack size. Differentiating with respect to the area A eqn (1) becomes [16]:

$$\frac{\partial W}{\partial A} = \left(\frac{\partial U^e}{\partial A} + \frac{\partial U^p}{\partial A}\right) + \frac{\partial \Gamma}{\partial \mathrm{A}}, \tag{3}$$

because $\frac{\partial(\bullet)}{\partial t} = \frac{\partial A}{\partial t}\frac{\partial(\bullet)}{\partial A}$ from chain rule.

The well known potential energy of the system Π is given by [14-16]:

$$\Pi = U^e - W \tag{4}$$

Then from eqn (3) it is obtained:

$$-\frac{\partial \Pi}{\partial \mathrm{A}} = \frac{\partial U^e}{\partial A} + \frac{\partial \Gamma}{\partial \mathrm{A}} \tag{5}$$

Eqn (5) results from the fact that rate of potential energy decreasing during crack growth is equal to the rate of the energy dissipated in plastic deformation and crack growth.

2-2 Griffith Theory

For an ideally brittle solid the energy dissipated in plastic deformation is negligible and can be omitted in eqn (3).If γ represents the energy required to form a unit of new material surface then eqn (3) becomes:

$$G = \frac{\partial W}{\partial A} - \frac{\partial U^e}{\partial A} = \frac{\partial \Gamma}{\partial \mathrm{A}} = 2\gamma \tag{6}$$

where the factor 2 appearing on the right hand side of the equation refers to the two new material surfaces formed during the crack growth. The left hand side of equation represents the energy available for crack growth and is given by the symbol G in honor of Griffith. Equation (6) represents the fracture criterion for crack growth. Two limiting cases the 'fixed-grips' and 'dead load loading' are usually encountered in practice. If the work of body forces is ignored the work performed by the applied loads vanishes and equation (6) results:

$$G = -\frac{\partial U^e}{\partial A} = 2\gamma \tag{7}$$

Eqn (7) shows that the magnitude of the elastic strain energy release rate in combination with equation (5) can be forms as:

$$G = -\frac{\partial \Pi}{\partial A} = 2\gamma \tag{8}$$

From eqn (8) we may have:

$$\frac{\partial(\Pi + \Gamma)}{\partial A} = 0 \tag{9}$$

which in Griffith's terminology states that the 'total potential energy' of the system is stationary. If a crack of length 2a is considered in an infinite plate subjected to a uniform stress σ perpendicular to the crack plane, the change in elastic strain energy due to the presence of the crack is given by [16,18] :

$$U^e = \frac{\pi a^2 \sigma^2}{8\mu}(\kappa + 1) \tag{10}$$

Where κ=3-4ν for plane strain and κ= (3-ν)/ (1+ν) for plane stress. Taking into consideration the crack area and introducing eqn (10) into (7), the critical stress required for an unstable crack growth is given by:

$$\sigma_c = \sqrt{\frac{2E\gamma}{\pi a(1-\nu^2)}} \tag{11}$$

for plane strain; and

$$\sigma_c = \sqrt{\frac{2E\gamma}{\pi a}} \tag{12}$$

for plane stress.

The load displacement response of a body of unit thickness with an initial crack of length a_1 for 'Fixed grips loading' is shown in Figure 2. During loading up to the point A, the elastic strain energy stored in the body is represented by the area *(OAC)*. Line OA and OB represents the load displacement response for a crack length α_1 and $\alpha_2=\alpha_1+\Delta\alpha$ respectively. During crack propagation the load drops from point A to point B. The slope of line OA and OB represents the stiffness of the body for a crack length a_1 and a_2 respectively. The energy release rate is given by:

$$G = \frac{(\mathrm{OAB})}{\Delta a} = 2\gamma, \tag{13}$$

where (OAB) is the area of the triangle OAB.

The load displacement response of a body of unit thickness with an initial crack of length a_1 for 'Dead loading' is shown in Figure 3.The displacement increases from A to B the crack length increases from a_1 to a_2 as above.

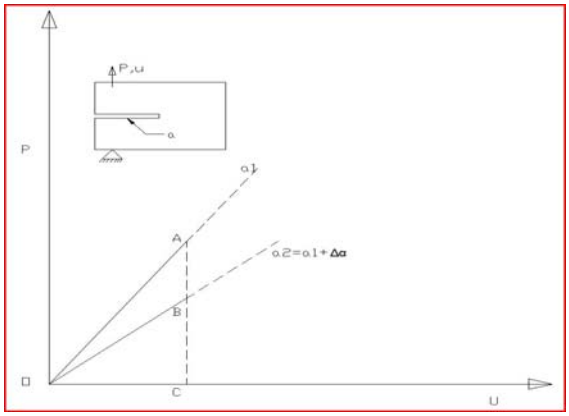

Figure 2: Load displacement response of a cracked plate from length a_1 to a_2 under 'fixed grips' conditions along AB

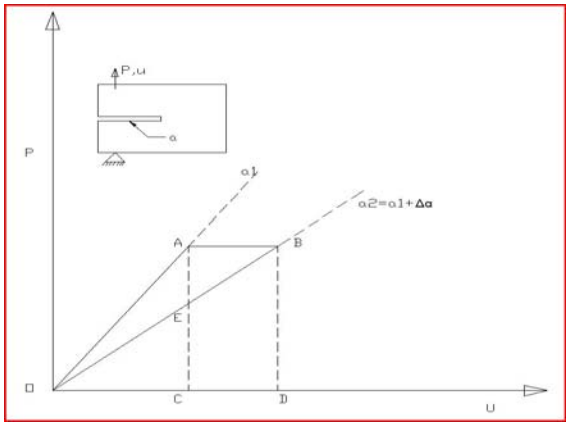

Figure 3: Load displacement response of a cracked plate from length a_1 to a_2 under 'fixed grips' conditions along AB

2-3 Graphical representation of the energy balance equation

The graphical representation of load displacement curve for fixed grip loading and dead load (constant load) displacement is given in Figure 2 and 3 respectively. Usually both load and displacement change during crack growth. The load displacement response during quasi-static growth of a crack of initial length a_1 το final crack length a_5 is represented by the curve A1A2A3A4A5 in Figure 4.The equation which express the crack driving force in terms of segmental areas of the load displacement curve is eqn (13).This allow to construct the P-u curve and draw the radial lines OAi which correspond to different crack lengths. Finally G is determined by [16] :

$$G = \frac{(\mathrm{OA}_i\mathrm{A}_j)}{a_j - a_i};\ i, j = 1,2,3,4,5 \tag{14}$$

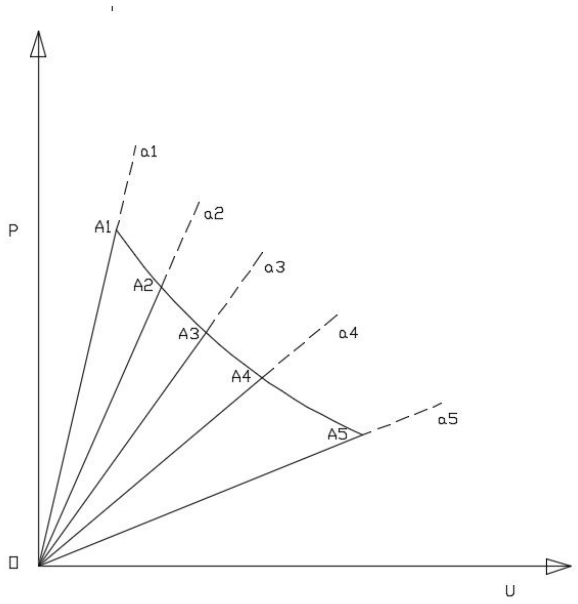

Figure-4: Load displacement response of a cracked plate for propagation of a crack from an initial length a_1 to a final length a_5 under load - displacement conditions along $A_1A_2A_3A_4A_5$

2.4 Equivalence between strain energy release rate and stress intensity factor

The relationship between the strain energy release rate, which is a global quantity, and the stress intensity factor, which expresses the strength of the local elastic stress field at the neighborhood of the crack tip, is very important. Let us consider the case of an opening mode where the crack extends along its own direction in a self similar manner. The energy release rate is given by [16]:

$$G_I = \frac{\mathrm{K_I^2}}{\mathrm{E}} \tag{15}$$

for generalized plane stress and

$$G_I = \frac{(1-\nu)\mathrm{K_I^2}}{\mathrm{E}} \tag{16}$$

for plane strain, where K_I the opening mode-I stress intensity factor.

The calculation of strain energy release rate G_{II} for mode II loading (sliding mode) is not easy, since the crack does not propagate in its own plane, but follows a curved path which is not known in advance. The energy release rate G_{II} for mode II in terms of K_{II} stress intensity factor is given by [16]:

$$G_{II} = \frac{(\kappa+1)\mathrm{K}_{\mathrm{II}}^2}{8\mu} \tag{17}$$

3 SOLUTION OF THE PROBLEM

3-1 Damage Initiation.

First it is introduced an uncracked sandwich model with identical boundary and loading conditions as the sandwich beam under consideration (Figure 1).The finite element model solved in Abaqus [15] is shown in Figure 5 and the results of the analysis in Figure-6.

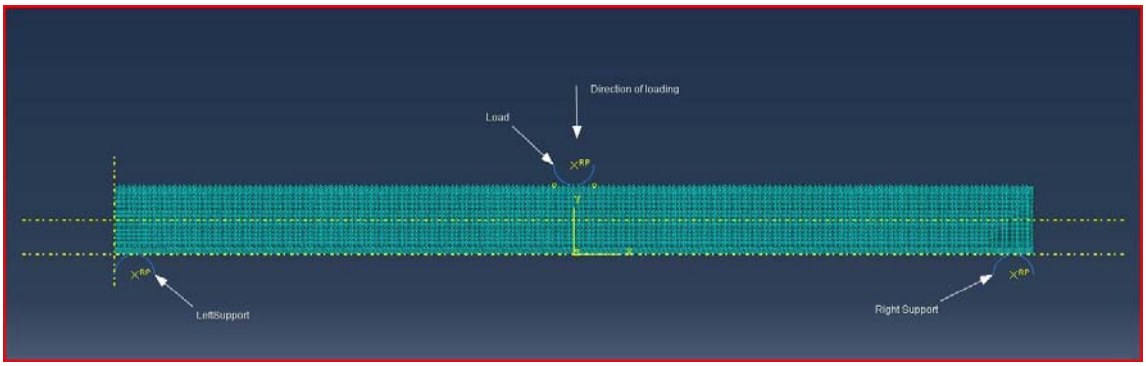

Figure-5: Finite Element model

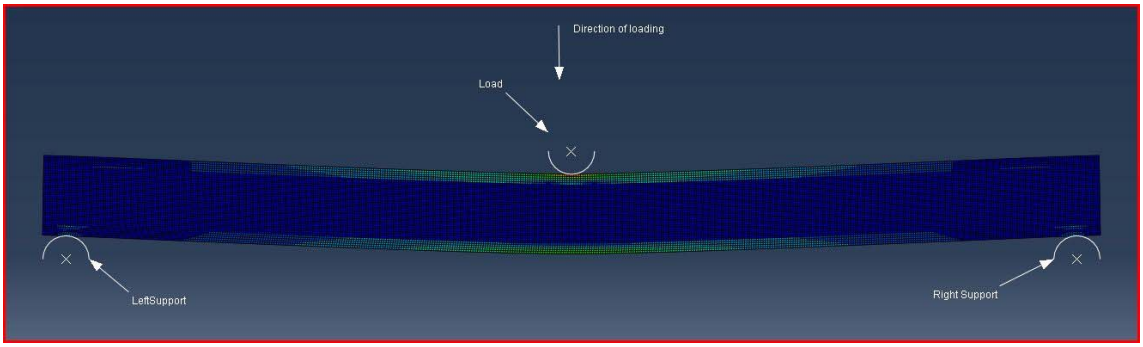

Figure 6: Solution of the Finite element analysis of the uncracked sandwich beam

Then we focus on a specific area where it is expected to begin a crack due to a gap or some other reason. This specific area is shown in Figure 7.

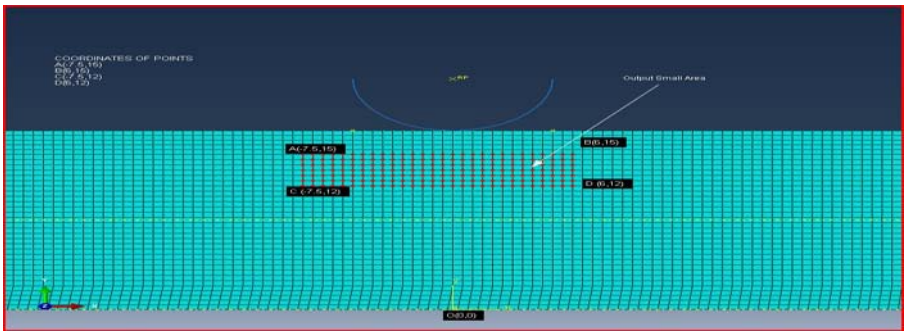

Figure 7: The specific area where we are waiting to start the initial damage and the cracking propagation

Then via a specific code in Matlab [19] it is analyzed the data of post processing in Abaqus and most specifically the V.Mises and Tresca equivalent stress distribution within this area. The spatial distribution of the

equivalent stresses, it is plotted in Figure 8.

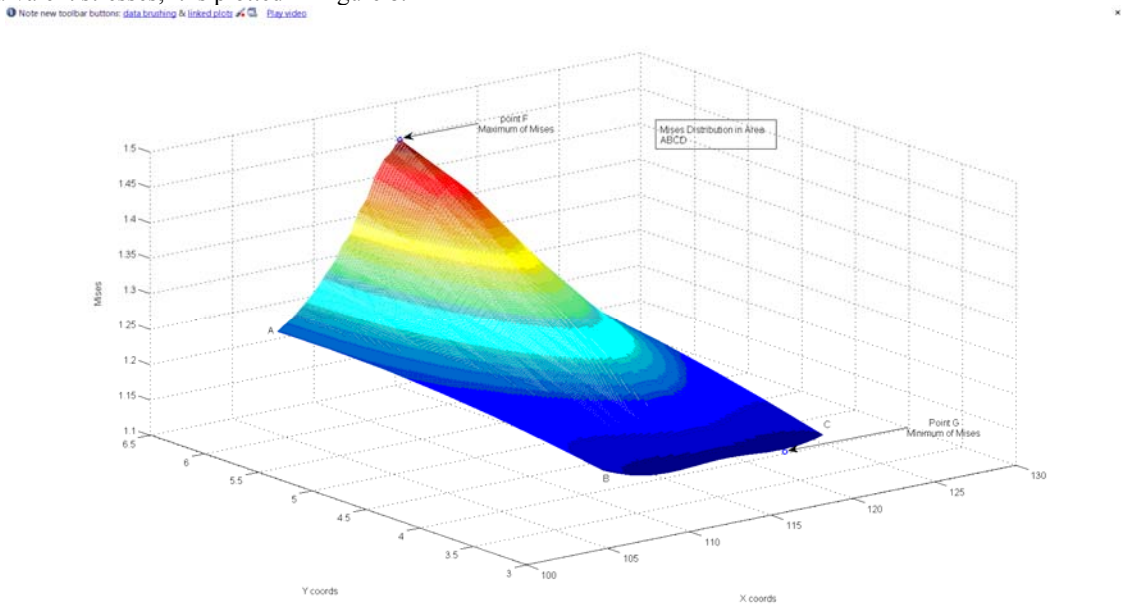

Figure 8: Mises Distruibution in area ABCD

3-2 Finite element model.

In order to estimate G_{Ic} using the before mentioned procedure in Section 2.3 we construct some FE models subjected in pure tensile tests with various crack lengths of a(mm) (2, 5, 10, 20, 30, 40, 50). For each length we make several runs in order to adjust the V.MISES equivalent stress just on the crack tip node very close to the yield stress of the material. Then, following the procedure described in 2.3 we estimate the G_{Ic} value which will be inserted as a material constant into the cohesive finite element model. A typical model is shown in Figure 9 in and the plotted diagrams of load-displacement curves in Figure 10.

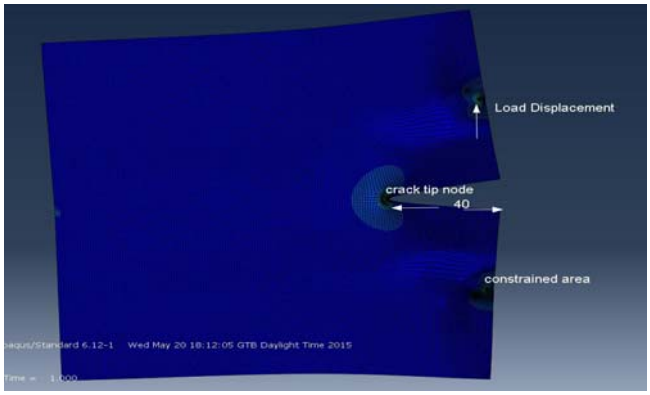

Figure 9: Finite Element model of a typical length 40mm subjected in pure tensile load.

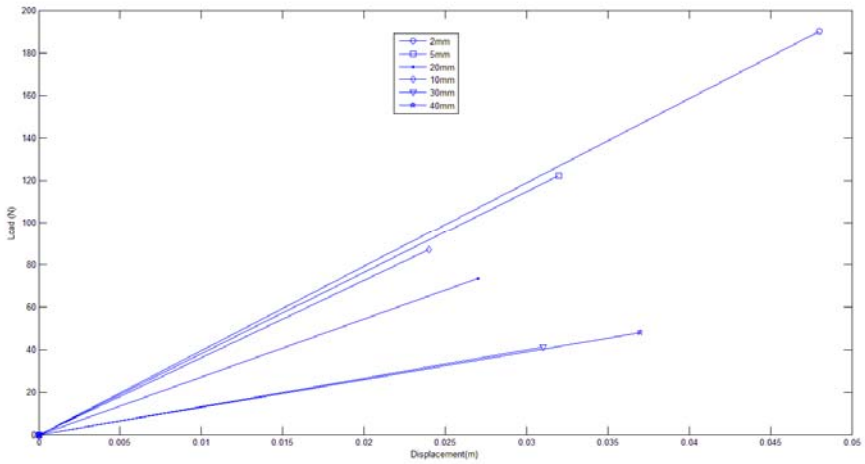

Figure 10: The Load Displacement curves of pure tensile numerical tests.

The method of calculation the G_{IIc} value is quite similar. Now the same model is subjected to pure shear and the load is adjusted such us the equivalent V.Mises. Stress on the crack tip reaches the yielding stress. Then, for each crack length we use relationship (17) and finally the average value is obtained. This is the second material parameter which will be inserted in cohesive model.

3-3 Cohesive model.

The building strategy of cohesive finite element model is briefly described in Figure 11.

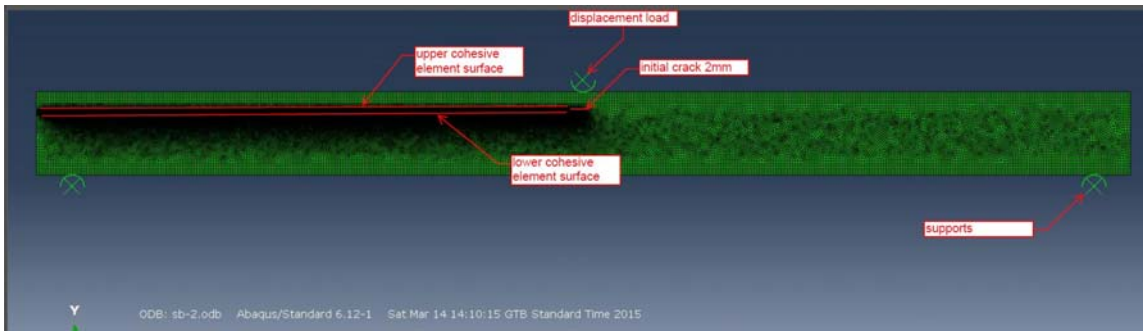

Figure 11: The Cohesive Finite Element Model.

A self contact analysis is running in parallel with the main cohesive analysis in order to prevent interpenetration between upper and lower cohesive element surface. In supports and loading positions we have inserted another contact analysis in order to simulate the real experimental conditions. The final result of running the aforementioned cohesive model is shown in Figure 12.

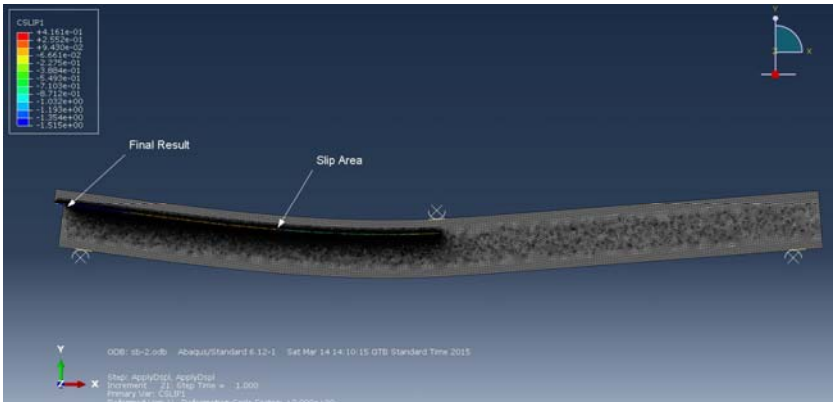

Figure 12: The cohesive finite element analysis

4 CONCLUTIONS

The cohesive finite element method does not predict the path of the crack advance. It only simulates the final collapse of the model. This is due to the modeling by the use of a prescribe crack path. In our analysis it has been chosen a path coincided and parallel with the initial crack just below the upper boundary of the core.

A loss in accuracy of the G_{Ic} calculation must happens because the tensile models yield a small value of K_{II} which indicates that there also are exist mode- II conditions and by that an inserted fault in the measurements.

A further analysis of special elements (XFEM) of Abaqus Library is needed in order to simulate the real cracking propagation. The G_{Ic} and G_{IIc} material properties will be inserted in a similar way.

This kind of model is extremely nonlinear because it includes 3 contact analyses between the supports and the body, a self contact analysis between the cohesive areas, and a cohesive analysis using the default cohesive law.

REFERENCES

[1] Carlsson, LA., Sendlein, L.S. and Merry, S.L. (1989), "Characterization of Face Sheet/Core Shear Fracture of Composite Sandwich Beams", *Journal of Composite Materials*, Vol. 25, pp. 101-116.

[2] Kulkarni, N., Mahfuz, H., Jeelani, S., and Carlsson, L.A. (2003), "Fatigue crack growth and life prediction of foam core sandwich composites under flexural loading", *Composite Structures*, Vol. 59, pp. 499-505.

[3] Berggreen, C., Simonsen, B.C. and Borum, K.K. (2007), "Prediction of debond propagation in sandwich beams under FE-bared Fracture Mechanics and NDI Techniques", *Journal of Composite Materials*, Vol. 41, pp. 493-520.

[4] Theotokoglou, E.E., Hortis, D., Carlsson, L.A. and Mahfuz, H. (2008), "Numerical study of fractured sandwich composites under flexural loading", *Journal of Sandwich Structures and Materials*, Vol. 10, pp. 75-94.

[5] Theotokoglou, E.E., Tourlomousis, I.I. (2010), "Crack kinking in sandwich structures under three point bending", *Theoretical and Applied Fracture Mechanics*, Vol. 30, pp. 158-164.

[6] Barrenblat, G.I. (1962), "The mathematical theory of equilibrium cracks in brittle fracture", *Advances in Applied Mechanics*, Vol. 7, pp. 55-129.

[7] Dugdale, D.S. (1960), "Yielding of sheets containing sheets", *J. Mech. Phys. Solids*, Vol. 8, pp. 100-104.

[8] Xu, X.P., Needleman A. (1994), "Numerical simulations of fast crack growth in brittle solids", *J. Mech. Phys. Solids*, Vol. 42, pp.1397-1434.

[9] de Morais, A.B., de Moura, M.F.S.F., Goncalves, J.P.M. and Camanho, P.P. (2003),"Analysis of crack propagation in double cantilever beam tests of multidirectional laminates", *Mechanics of Materials*, Vol. 35, pp. 641-652.

[10] Sorensen, B.F., Kirkegaard, P. (2006), "Determination of mixed mode cohesive laws", *Engineering Fracture Mechanics*, Vol. 73, pp. 2642-2661.

[11] Kyoungsoo, P., Paulino, G.H. and Roesler, J.R. (2009), "A unified potential-based cohesive model of mixed-mode fracture", *J. Mech. Phys. Solids*, Vol. 57, pp. 891-908.

[12] Ramantani, D.A., de Moura, M.F.S.F., Campilho, R.D.S.G., and Marques, A.T. (2010), "Fracture characterization of sandwich structures interfaces under mode I loading", *Composites Science and Technology*, Vol. 70, pp. 1386-1394.

[13] Ramantani, D.A., Campilho, R.D.S.G., de Moura, M.F.S.F. and Marques, A.T. (2010), "Stress and failure analysis of repaired sandwich composite beams using a cohesive damage model", *Journal of Sandwich Structures and Materials*, Vol. 12, pp. 369-390.

[14] El- Sayed S., Sridharar S. (2002), "Cohesive layer models for predicting delamination growth and crack kinking in sandwich structures", *Int. J. Fracture*, Vol. 117, pp. 63-84.

[15] Hibbit, Karlsson and Sorensen, Inc. (1999), Abaqus/Standard and Abaqus/Explicit version 5.8, Pawtucket, USA.

[16] Sih, G. C. (1974), "Strain energy density factor applied to mixed mode crack problems", *Int Journal Fracture Mech,* Vol. 10, pp. 305-321.

[17] Erdogan, F., Sih, G. C. (1963), "On the extension in plates under plane loading and transverse shear", *Journal Basic Eng*, Vol. 85, pp. 519-527.

[18] Gdoutos E.E. (1993), Fracture Mechanics an Introduction, Kluwer Academic Publishers.

[19] MatLab, TheMathWorks, Inc@ 1984-2014.

.